Meng *et al. Geoscience Letters* (2024) 11:13
https://doi.org/10.1186/s40562-024-00331-z

Geoscience Letters

RESEARCH LETTER
Open Access

Extreme precipitation trends in Northeast China based on a non-stationary generalized extreme value model

Fangxiu Meng[1†], Kang Xie[2†], Peng Liu[3*], Huazhou Chen[4], Yao Wang[1] and Haiyun Shi[1*]

Abstract

Northeast China is the main food production base of China. Extreme precipitation (EP) events can seriously impact agricultural production and socioeconomics, but the understanding of EP in Northeast China is still limited. In this study, using the non-stationary generalized extreme value (GEV) model, we investigate the trend and potential risk of EP in Northeast China during 1959–2017, especially in early and mid-summer (periods of high frequency of EP). Then, the relationships between EP and large-scale circulation over Northeast China in early and mid-summer are analyzed separately. The EP in Northeast China mainly presents positive trends in early summer but negative trends in mid-summer. Meanwhile, the EP with all the return periods presents apparently increasing trends in early summer, corresponding to more frequent EP events. Nevertheless, in mid-summer, the EP with 2-year return period decreases with location parameter, and the EP with 20-year, 50-year, and 100-year return periods slightly increases with scale parameter. The EP with 2-year return period occurs frequently in Liaoning Province, while the EP with 100-year return period is more likely to occur in Jilin Province and Heilongjiang Province. Moreover, the increase of the EP in early summer is mainly influenced by the northeast cold vortex; the effect of cold air on the EP is stronger in mid-summer, giving a clear explanation why the EP in mid-summer does not increase significantly. Overall, the outcomes of this study would be beneficial for the disaster prevention and mitigation in Northeast China.

Introduction

According to the Sixth Assessment Report of the Intergovernmental Panel on Climate Change (IPCC), the past 20 years have been the warmest period since the early twentieth century. The global warming rate over the last 50 years (since the 1970s) is greater than that of any other 50-year period in the last 2000 years. With global warming, extreme heat events (including heat waves) will become more frequent and intense, while extreme cold events will decrease and weaken at the global and continental scales. In addition, heavy precipitation events have become stronger and more frequent, resulting in increased flood and waterlogging compound events in some coastal and estuarine areas (Fan et al. 2021; IPCC 2021; Zhou and Qian 2021). Such extreme events can cause significant loss of life and property. Therefore, studying the trends and the occurrence probabilities of

[†]Fangxiu Meng and Kang Xie contributed equally to this work.

*Correspondence:
Peng Liu
liupeng1998@nuist.edu.cn
Haiyun Shi
shihy@sustech.edu.cn
[1] Shenzhen Key Laboratory of Precision Measurement and Early Warning Technology for Urban Environmental Health Risks, School of Environmental Science and Engineering, Southern University of Science and Technology, Shenzhen, Guangdong, China
[2] School of Mathematics and Information Sciences, Nanjing Normal University of Special Education, Nanjing, China
[3] School of Atmospheric Sciences, Nanjing University of Information Science and Technology, Nanjing, China
[4] College of Science, Guilin University of Technology, Guilin, China

extreme events is instructive for improving the forecasting and early warning capabilities of extreme events and mitigating disaster risks.

Many studies have shown clear increasing trends of extreme precipitation (EP) in the United States, Australia, China, India, and other regions (Suppiah and Hennessy 1998; Groisman et al. 2001; Roy and Balling 2004; Liu et al. 2005; Chen and Chu 2014; Hartmann and Buchanan 2014; Guan et al. 2022; Wang et al. 2022; Jiang et al. 2023). For instance, Chen et al. (2014) identified positive trends of EP in the Island of Hawaii and found a positive relationship between EP and the Southern Oscillation Index (SOI), implying more extreme events during La Nina years. Hartmann and Buchanan (2014) found that significant increasing trends in EP were detected in the mountainous regions in the east and north of the Indus River basin, which was influenced by the western disturbance transporting moisture from the Mediterranean and the Atlantic Ocean. Wang et al. (2022) indicated obvious increasing trend of extreme rainfall in the middle and lower reaches of the Yangtze River basin, and the extreme rainfall had a significant correlation with the large-scale climate patterns. In addition, there are spatial differences in the EP even in the same river basin. For example, the EP over the western part of the Indus River basin exhibited a decreasing trend; on the contrary, the EP in the east and north of the Indus River basin presented a noticeable increasing trend (Hartmann Hartmann and Buchanan 2014). The trend in the EP had been studied by multiple extreme indexes. Sheikh et al. (2015) showed that the trends of various extreme indexes in the Indo-Gangetic Plain could be quite different. Ren et al. (2017) and Zilli et al. (2017) showed that the trend in rainy days is decreasing in Southwest China, Myanmar, and large urbanized areas of Sao Paulo State. Han et al. (2005) reported that summer precipitation in Northeast China showed a decreasing trend with interannual variability periods of 14 years and 2–4 years. Therefore, it is particularly important to investigate the EP trend in different regions.

Moreover, most previous studies on precipitation in China focused on precipitation anomalies at the national scale or in southern China. Relatively few studies focused on the summer EP in Northeast China, especially in early summer and mid-summer. The terrain in Northeast China is flat, fertile, and sparsely populated, making it suitable for large-scale mechanical planting. This region has abundant sunshine, suitable temperature, and sufficient precipitation (over 70% of the annual precipitation), especially in summer, making it the main area for grain. As one of the most important food production bases in China, Northeast China is of great importance to national food security. Summer is the critical period for crop growth in Northeast China and the concentration of EP in this region. According to Shen et al. (2011) and Wu et al. (2021), the seasonal variation of precipitation from May to June is not consistent with that from July to August, so it is necessary to divide these months into early summer and mid-summer. In recent years, the EP events have occurred frequently in Northeast China, which have a serious impact on agricultural production and social life. For example, the highest 1-day precipitation record (more than 135 mm) in Jilin Province on July 28, 2010 caused the direct economic losses of more than 6.6 billion RMB. In the same year, there were 24 floods in Liaoning Province. Among them, heavy precipitation occurred 6 times (Li et al. 2012). According to the statistics of the 2012 climate disaster bulletin of Liaoning Province, four regional rainstorms successively occurred in 2012, of which the flood on August 4 was the most serious one. Based on the statistics of the National Disaster Reduction Center of China, some areas of Northeast China have been hit by heavy precipitation since September 2018, resulting in 100 thousand mu of affected crops and more than 9 billion RMB of economic losses. Consequently, a comprehensive analysis of the long-term spatiotemporal trends and the potential risks of the summer EP in Northeast China is of strategic significance for future development of food production bases in Northeast China and the guarantee of national food security.

The extreme value model was widely used in meteorology and hydrology studies to analyze the statistical characteristics of extreme events (Kharin and Zwiers 2005; García et al. 2007; Katz et al. 2013; Chen and Chu 2014; Tan and Shao 2017; Xavier et al. 2020; Zhang et al. 2020; Wu et al. 2021). The EP is obtained using the Annual Maxima (AM) method. Studies have shown that the GEV model was the optimal distribution for most EP obtained by the AM method in China, and such conclusion has been recognized by the World Meteorological Organization (World Meteorological Organization 2009; Du et al. 2020). The Generalized extreme value (GEV) model was used not only to fit the distribution of EP, but also to focus on its tail characteristics. Furthermore, the relationships between climate indexes and extreme events were discussed by considering the introduction of additional climate indexes in the non-stationary GEV model (Chen and Chu 2014; Tan and Shao 2017; Wu et al. 2021; Zhang et al. 2020). According to the non-stationary GEV model (changing with time), the return levels of extreme events were estimated and utilized to investigate the trends of future EP. It was also observed that the change of the EP was related to the location and scale parameters (Kharin and Zwiers 2005; García et al. 2007; Chen and Chu 2014; Xavier et al. 2020). However, there has been less comprehensive assessment of the risk evolution of

EP from multiple perspectives, including the spatiotemporal variations of EP with multi-year return period and the probabilities of occurrence of rainstorm, heavy rainstorm, and the precipitation larger than the regional average. Currently, methods such as the Mann–Kendall test, Sen's slope, and empirical orthogonal functions (EOF) analysis are predominantly used to analyze the trends of EP in Northeast China (Wang et al. 2013; Guo et al. 2019; Yu and Ma 2022). In this paper, the MK trend analysis method is used to the trend testing and mutation detection of EP in Northeast China. Further analysis of the spatiotemporal changes, future trends, and risk evolution of EP in Northeast China is conducted from a new perspective of the non-stationary GEV model. Additionally, the effects of the non-stationary GEV model parameters on the return levels are examined. These findings can help to understand the trend and occurrence probability of EP over Northeast China in early and mid-summer and can provide a reference for risk management.

Study area and data sources

The study area is Northeast China, located in the region of 38° N–53° N, 115° E–135° E (Fig. 1), including Liaoning Province, Jilin Province, Heilongjiang Province, and Hulun Buir City, Hinggan League, Tongliao City, and Chifeng City of the eastern Inner Mongolia (Du et al. 2013; Wu et al. 2021). Northeast China locates in the middle-high latitudes on the eastern coast of Eurasia, and its climate belongs to the temperate monsoon climate. It is one of the most sensitive regions to global climate change. The spatial–temporal distributions of EP in Northeast China are highly variable.

The daily precipitation records from 116 meteorological stations in Northeast China during 1951–2017 have been obtained from the National Meteorological Information Center of China Meteorological Administration. Since the non-stationary GEV model requires complete data records over a long time period, to preserve as many sites as possible, the following data quality control principles are formulated: if the proportion of the missing data from a meteorological station exceeds 5% within a year, the data in that year will be deleted; if the total missing measurement ratio of a meteorological station exceeds 5% of the total records, the data from that station will be deleted. In case the percentage of the missing data is less than 5%, we compare the data from one station with nearby stations with complete records and check the abnormal values (Chen et al. 2014). If there are no abnormal values, the missing data shall be supplemented by the historical mean value of the same period. For the abnormal value, we confirm the authenticity of the abnormal value by looking up the data. If it is not true, we replace the abnormal data with the historical mean value of the same period. Finally, the data from 107 stations during

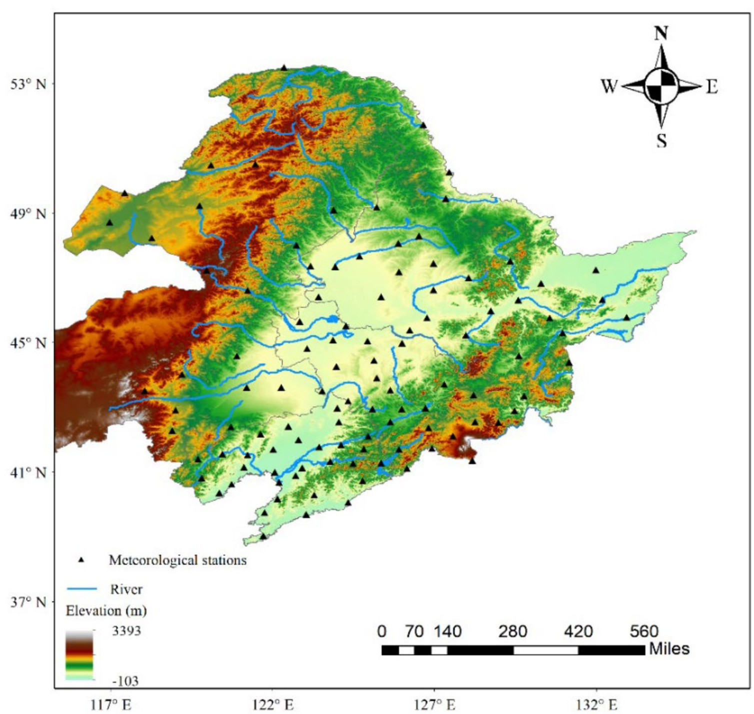

Fig. 1 Spatial distribution of the meteorological stations over Northeast China

1959–2017 are used in this study to ensure data consistency and completeness. Previous studies on the EP in Northeast China mostly focused on the whole summer (Han et al. 2005). However, Shen et al. (2011) pointed out that the intra-seasonal variability of EP is noticeable during summer. Therefore, this study focuses on two periods, i.e., early summer (May and June) and mid-summer (July and August), and defines the EP as the maximum 24-h accumulated precipitation during each period (Gao et al. 2016; Jeon et al. 2016; Tan and Shao 2017; Zhang et al. 2020).

Methods

The EP variability is investigated by using the MK trend analysis method. Additionally, a non-stationary GEV model is adopted to analyze the trends and potential risks of the EP in Northeast China.

Mann–Kendall trend analysis method

The Mann–Kendall (MK) trend analysis method, first proposed by Mann (1945) and implemented by Kendall (1975), is widely used in trend testing and mutation detection. It does not require a fixed data distribution and is not disturbed by a few outliers. In addition, it also does not require high data quality. This method, which is recommended by the World Meteorological Organization (WMO), has been widely used for trend analysis in hydrology and meteorology (Wei 2007; Shi et al. 2017; Zhou et al. 2020; Jiang et al. 2021). The specific steps are shown as follows:

For the EP $X = \{x_1, x_2, x_3 \cdots x_n\}$, an ordered series can be constructed as Eq. (1):

$$S_k = \sum_{i=1}^{k} r_i \quad (k = 2, 3, \ldots, n), \tag{1}$$

where r_i can be calculated by Eq. (2):

$$r_i = \begin{cases} 1, & \text{if} x_i > x_j \\ 0, & \text{otherwise} \end{cases} \quad (j = 1, 2, \ldots, i), \tag{2}$$

where r_i denotes the number of times when the value at time i is greater than that at time j. S_k indicates the cumulative value of r_i. Assuming that the time series S_k is randomly independent, the statistic can be defined as Eq. (3):

$$\mathrm{UF}_k = \frac{S_k - E(S_k)}{\sqrt{\mathrm{Var}(S_k)}} \qquad (k = 1, 2, \ldots, n), \tag{3}$$

where $\mathrm{UF}_1 = 0$, and $E(S_k)$ and $\mathrm{Var}(S_k)$ represent the mean and variance of S_k, respectively. Assuming that $x_1, x_2, x_3 \cdots x_n$ are independent of each other and have the same continuous distribution, $E(S_k)$ and $\mathrm{Var}(S_k)$ can be calculated by Eqs. (4) and (5):

$$E(S_k) = \frac{n(n-1)}{4}, \tag{4}$$

$$\mathrm{Var}(S_k) = \frac{n(n-1)(2n+5)}{72}. \tag{5}$$

The significance of the trend is tested by using UF_k value. Generally, positive UF_k value represents an upward trend, and negative value means an upward trend. The trend is considered significant if the absolute value of UF_k is greater than 1.96. Then, we repeat the above procedure for the time series in reverse order, i.e., $\{x_n, x_{n-1}, x_{n-2}, \cdots, x_1\}$, and calculate the statistic UB_k to make the UB_k equal to $-\mathrm{UF}_k$. Based on the intersection points of the UF and UB curves, the mutation years are detected.

Non-stationary GEV model

According to the definition of extreme events, if the EP represented by $\{y_1, \ldots, y_N\}$ is independently and identically distributed with a common cumulative distribution function, $M_n = \max\{y_1, \ldots, y_N\}$ obeys one of three distributions, i.e., Gumbel, Fréchet, and Weibull distributions. We refer to these three distributions collectively as the GEV distribution (Coles 2001):

$$F(m) = \exp\left\{-\left[1 + \xi\left(\frac{m-\mu}{\sigma}\right)\right]^{-1/\xi}\right\}, 1 + \xi\left(\frac{m-\mu}{\sigma}\right) > 0, \tag{6}$$

where μ, σ (>0), and ξ indicate the location, scale, and shape parameters, respectively. Positive, zero, and negative values of the shape parameter represent different distributions.

The assumption of stationarity used in EP is highly uncertain due to the influence of climate change and human activities. Therefore, this study constructs non-stationary GEV models with time-varying location and scale parameters to analyze the variation trends of the EP. The five common types of non-stationary GEV model are shown in Table 1. According to the principle of the minimum Akaike Information Criterion (AIC) value, the best-fit models for the EP are selected under non-stationary

Table 1 Trend types of non-stationary GEV model

Trend types	Parameter forms
μ linear trend, σ no trend (AL)	$\mu(t) = \mu_0 + \mu_1 t, \sigma(t) = \sigma_0$
μ parabolic trend, σ no trend (AP)	$\mu(t) = \mu_0 + \mu_1 t + \mu_2 t^2, \sigma(t) = \sigma_0$
μ no trend, σ linear trend (BL)	$\mu(t) = \mu_0, \sigma(t) = \sigma_0 + \sigma_1 t$
μ no trend, σ parabolic trend (BP)	$\mu(t) = \mu_0, \sigma(t) = \sigma_0 + \sigma_1 t + \sigma_2 t^2$
μ linear trend, σ linear trend (DL)	$\mu(t) = \mu_0 + \mu_1 t, \sigma(t) = \sigma_0 + \sigma_1 t$

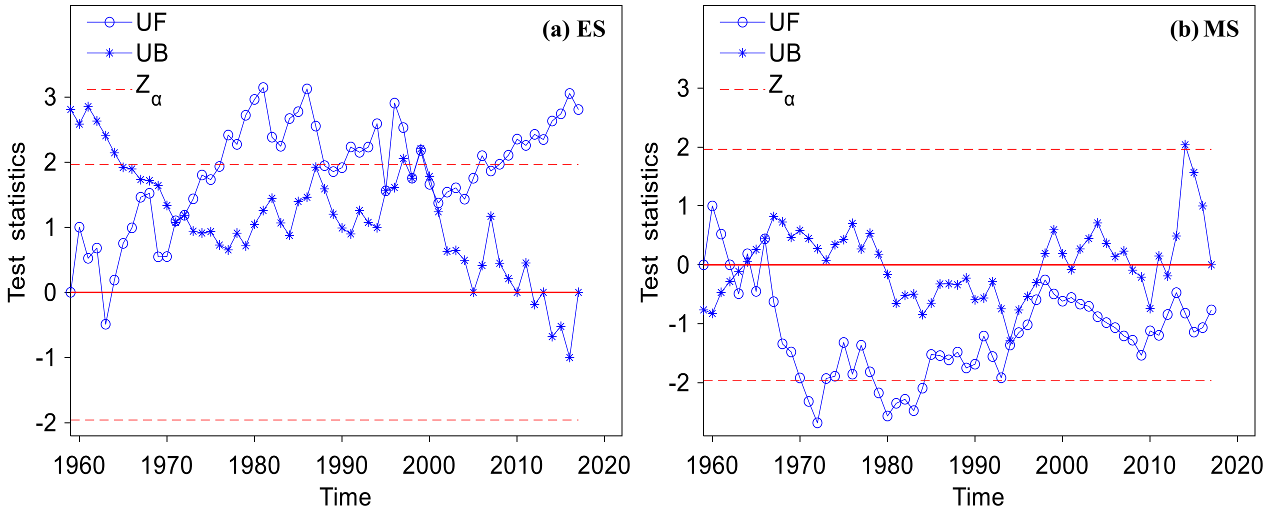

Fig. 2 The MK trend analysis method of the EP in Northeast China in **a** early summer (ES) and **b** mid-summer (MS). UF is the MK trend analysis method statistic of positive order. UB is the MK trend analysis method statistic of reverse order. Z_α represents the 95% percentile value of the standard normal distribution. The solid red line represents a horizontal line, indicating that there is no trend in the sequence. The red dashed line represents 95% confidence level

conditions, and the time-varying trend types of the location and scale parameters are determined. The significance of non-smooth effects was tested further through a likelihood ratio test.

The EP with T-year return period

The EP with T-year return period is defined as the reciprocal of P, i.e., $P = \frac{1}{T}$, which is the probability of exceeding the annual extremes in any given year. It is often referred to as a T-year event in hydrology (Filliben 1975; Coles 2001). The relationship between the return period (T) and the associated return level (x_T) can be expressed as Eq. (7):

$$F(x_T) = P\left(M_y \leq x_T\right) = 1 - \frac{1}{T}, \tag{7}$$

where x_T denotes the $(1 - \frac{1}{T})$ quantile of the EP probability distribution for any year, and M_y represents the EP.

Based on the best-fit models for the EP, the time-varying T-year return level x_T is obtained by Eq. (8):

$$x_T = \mu - \frac{\sigma}{\xi}\left[1 - \left\{-\log\left(1 - \frac{1}{T}\right)\right\}^{-\xi}\right]. \tag{8}$$

Results and discussion

Trends in the EP

Through the MK trend analysis method, the significance test for the EP trends in Northeast China is performed at the 0.05 significance level (Fig. 2). According to the UF curve, in early summer, the EP shows a significant increasing trend since the 1970s. Especially after the 1980s, the EP trend is more evident, which passed the significance test at the 99% confidence level. On the contrary, since the 1960s, a significant decreasing trend dominates the EP in mid-summer. Especially from the 1970s to the 1990s, the EP trend is more significant at the 0.01 significance level. Based on the intersection points of the UF and UB curves, it is determined that the EP increase in early summer shows a mutation from 1972 to 1995. The increasing trends in the EP are more evident after the mutation in 1972 and slightly decrease after the mutation in 1995. The EP decrease in mid-summer also presents a mutation, especially from 1966 to 1998. The slopes of the EP reduction increase after a sudden change in 1966 and become smooth after 1998. These results are highly similar to previous studies (e.g., Lin et al. 2021).

The spatial distributions of the EP trends in Northeast China in early summer and mid-summer are shown in Fig. 3. As is seen, the EP values at 90 stations show increasing trends in early summer. The number of stations with increasing EP trends approximately accounts for 84.11% of all stations. In particular, there are 13 stations with increasing EP trends that are significant at the 0.05 level and even have passed the test at the 99% confidence level. These stations are mainly located in Liaoning, Jilin, and Heilongjiang Provinces. Among them, the stations with a significant increase in the EP are mostly located in Heilongjiang Province, especially in the Songhuajiang and Nenjiang River Basin, where precipitation is abundant. In mid-summer, decreasing trends prevail at 53 stations. The numbers of stations with the

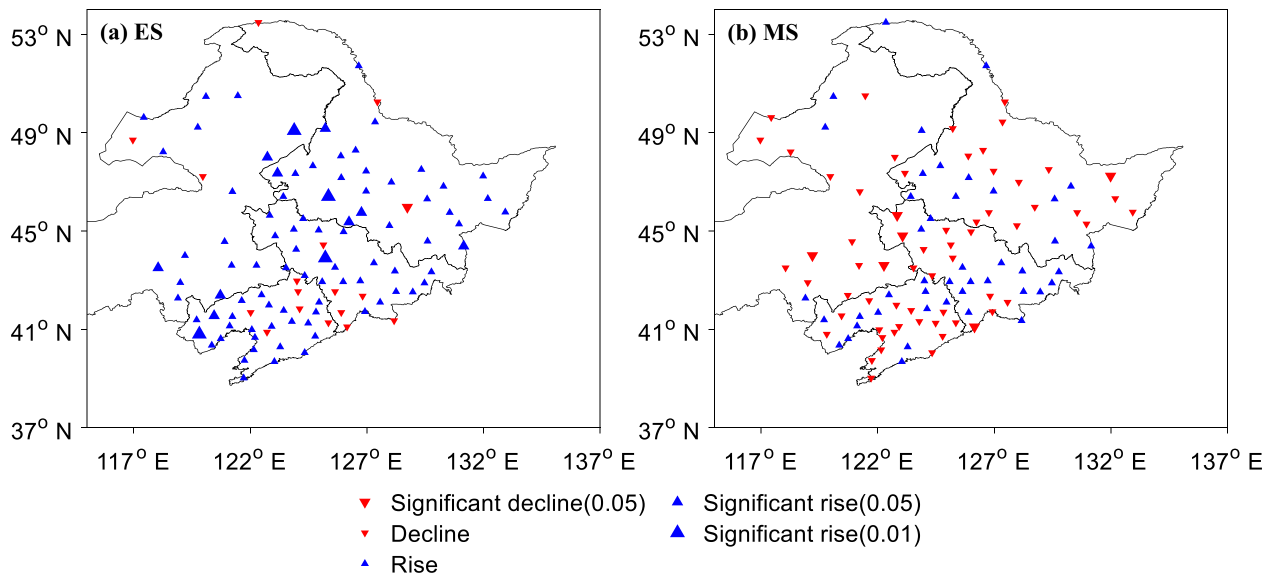

Fig. 3 Spatial distribution for the EP trends by using the MK trend analysis method in **a** early summer (ES) and **b** mid-summer (MS). The blue triangle represents an upward trend, while the red triangle represents a downward trend

decreasing EP trends and increasing EP trends are similar. However, the upward EP trends have not passed the significance test. The decreasing EP trends in Tongliao City and northwestern Jilin Province are significant at the 0.05 level, and these regions are located in the Liaohe and Songhua River basins.

The EP trends obtained from the non-stationary GEV model

Trends in the non-stationary GEV parameters

The MK trend analysis method examines the trend changes and confirms the non-stationarity of the EP in Northeast China during the summer. Additionally, the trend change of EP in Northeast China is investigated from a new perspective of the non-stationary GEV model. The spatial distributions of the trends in the location and scale parameters are shown in Fig. 4. Among them, the location parameter u_1 corresponds to the mean value of the EP, while the scale parameter σ_1 represents the variance of the EP. The trend of the EP is mainly influenced by u_1. In early summer, these two parameters present predominantly positive trends, corresponding to the enhancement of the EP. The likelihood ratio test verified the non-stationarity of the EP. Based on the results of the likelihood ratio test, the u_1 is positive at about 82.24% of all the stations. Among them, the u_1 trend is significantly positive at the 0.05 level at 22.73% of all the stations, and these stations are mainly located in the southwest of Liaoning Province, Tongliao City, the northwest of Jilin Province, and the south of Heilongjiang Province. In mid-summer, the trend of u_1 is not obvious or slightly decreases, corresponding to the decline of the EP. The u_1 shows negative trends in Tongliao City, northwestern Jilin Province, and central Heilongjiang Province, which have passed the significance test at the 0.05 level. These spatial and temporal results are highly similar to the EP trends obtained from the MK trend analysis method (Figs. 2, 3). The σ_1 responds to the inherent variability of EP. The trends of σ_1 and u_1 are not always the same, and the trend behavior in σ_1 shows a positive trend in early and mid-summer. In early summer, the σ_1 at 92 stations shows a positive trend. In particular, there is a significant increase in 35 stations, and these stations are also mainly located in southwestern Liaoning Province, Tongliao City, northwestern Jilin Province, and central Heilongjiang Province. These regions exhibit an increasing trend in EP, with a high inherent variability. It is recommended to flood control design of water conservancy at the highest level. In mid-summer, the σ_1 presents a positive trend in northern and southern Liaoning Province (especially in the Liaohe River Basin), northwestern and southern Jilin Province, and central Heilongjiang Province.

Trends in the EP with different return periods

Figure 5 shows the time series of the EP with 2-, 20-, 50-, and 100-year return periods in Northeast China in early summer and mid-summer, which are obtained by transforming the standardized data back to the original space. Results show that the EP in Northeast China are non-stationary in early summer, but not obvious in mid-summer.

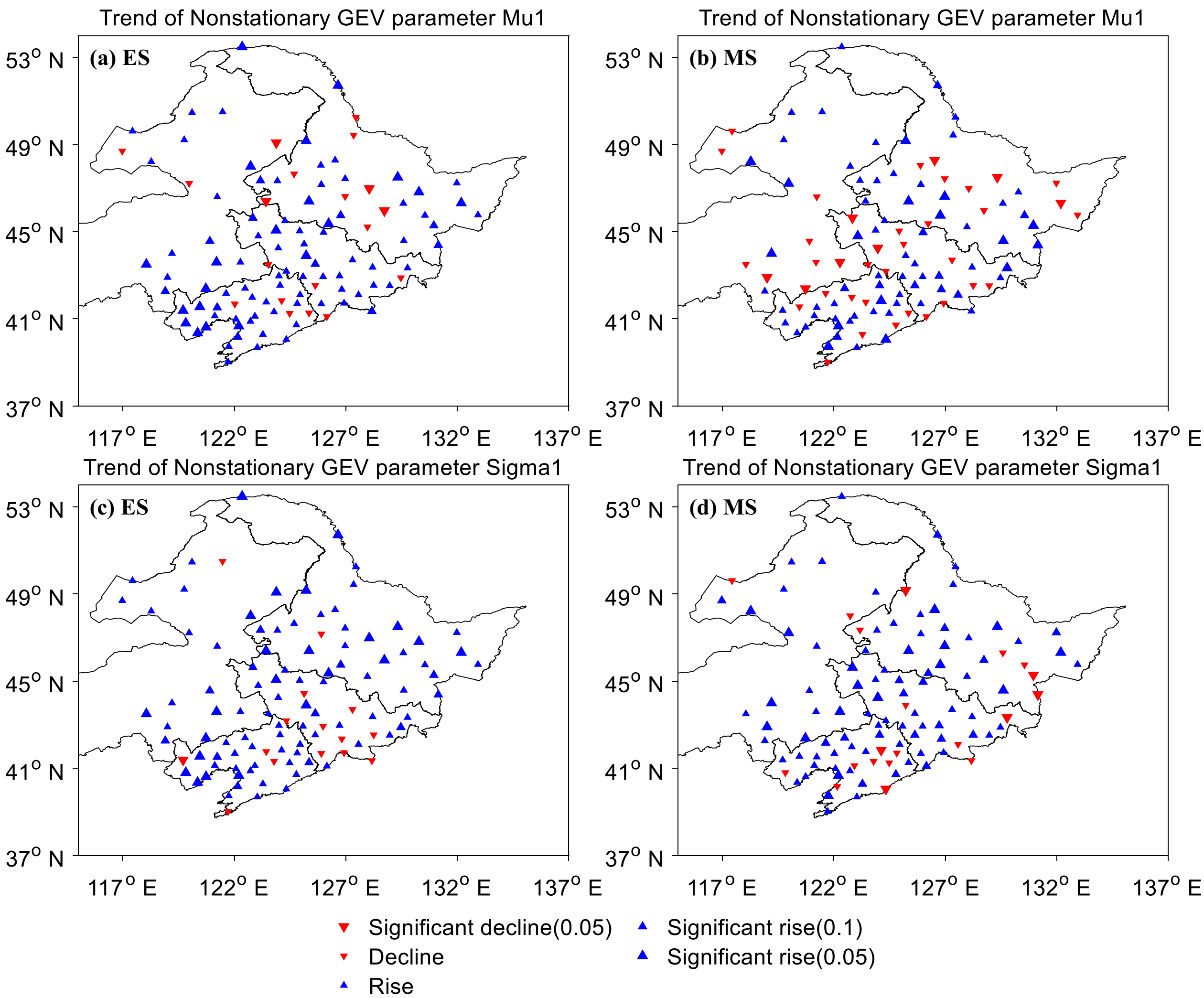

Fig. 4 Spatial distributions of the trends in location parameter u_1 and scale parameter σ_1 for the EP in Northeast China in **a**, **c** early summer (ES) and **b**, **d** mid-summer (MS). The blue triangle represents an upward trend, while the red triangle represents a downward trend

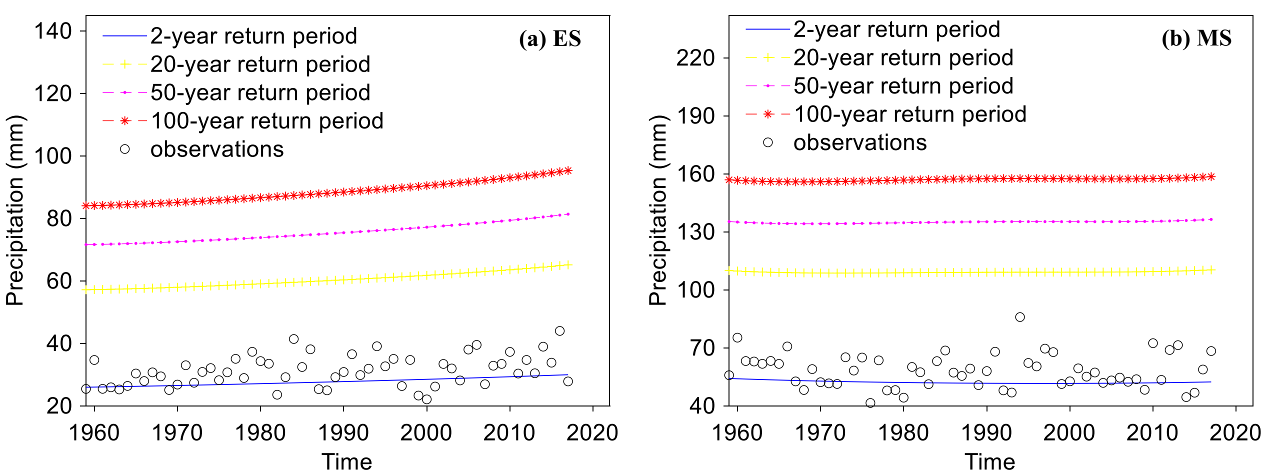

Fig. 5 Time series of the EP with 2-, 20-, 50-, and 100-year return periods in **a** early summer (ES) and **b** mid-summer (MS). Straight lines represent time series with different return periods, while scatter points mean the EP

Specifically, the different return periods (20-, 50-, and 100-year) show clear increasing trends in early summer, accompanied by slight increasing trends during mid-summer, and the EP with 100-year return period increases at the highest rate. Particularly, in early summer, it increases from 84.05 mm in 1969 to 95.31 mm in 2017, with a linear variability of 1.9 mm per 10 years. The EP events are more frequent, especially in early summer. For instance, the EP with a probability of 1/100 in 1959 only has a probability between 1/51 and 1/52 in 2017. Similarly, the EP with 50-year return period in 1959 has become relatively common (22–23 years) in 2017. The EP with 2-year return period is relatively stable in both periods, showing slight increase in early summer with a linear variability of 0.69 mm per 10 years. Nevertheless, in mid-summer, there is a slightly decreasing trend in the EP with 2-year return period. Specifically, the EP with 2-year return period increases from 25.96 mm in 1959 to 29.96 mm in 2017 in early summer. While in mid-summer, it decreases from 54.17 mm in 1959 to 52.38 mm in 2017. According to Fig. 4, when both location parameter u_1 and scale parameter σ_1 have positive trends, the return level increases with the growth of return period. Therefore, in early summer, the growth rates of the EP with 20-, 50-, and 100-year return periods are greater than that of the EP with 2-year return period. However, when location parameter u_1 shows a negative trend and scale parameter σ_1 displays a positive trend, the trends in the return levels are not the same. There is a slightly decreasing trend in the EP with 2-year return period, while that for the EP with 20-, 50-, and 100-year return periods slightly increase. This phenomenon is caused by the different trends in these two parameters. The location parameter u_1 has a major effect on the EP with 2-year return period, while the scale parameter σ_1 contributes more to the EP with 20-, 50-, and 100-year return periods. The relationships of the EP changes with the scale and location parameters have been studied in Northeast China for the first time, and these results are highly similar to previous studies in other regions (Kharin and Zwiers 2005; García et al. 2007; Chen and Chu 2014; Xavier et al. 2020).

Furthermore, the trends in the common EP (i.e., the EP with 2-year return period) and rare EP (i.e., the EP with 100-year return period) are tested by the MK trend analysis method (Fig. 6). The results suggest that, in early summer, the common EP and the rare EP both show significant increasing trends, and the spatial distributions of the EP trends are consistent. However, in mid-summer, there is no remarkable difference in the number of stations between decreasing EP trends and increasing EP trends. During early summer, 76.64% of stations show an increasing trend in the common EP, among which 90.24% are significant at the 99% confidence level. The difference is very small between the number of stations with decreasing EP trends and increasing EP trends. Approximately 50.47% of stations show decreasing trends, among which 85.19% are significant at the 99% confidence level. The rare EP increases significantly at 53 stations, which are located in Liaoning Province, central Jilin Province, Heilongjiang Province, Tongliao City and Hulun Buir City, i.e., the Liaohe, Mudanjiang, and Nengjiang River basins, where precipitation is abundant. The spatial distribution of the common EP trends is consistent with that of the rare EP. However, there are significant spatial variations in the Sen's slope among them. In general, the common and rare EP over Northeast China show significant increasing trends in early summer, and most of Northeast China faces an increasing trend in the EP risk, indicating that the EP events would become more frequent (Fig. 5). However, in mid-summer, this trend is not obvious. The expanded scope has reduced. It is necessary to focus on these stations, which are located in the Bohai Sea, Liaohe River and Songhua River basins, and strengthen the precautions against the EP impacts.

Potential risk of the EP in Northeast China

Using the non-stationary GEV model, we assess the potential risks of the common EP and the rare EP to cause rainstorm, heavy rainstorm, and the precipitation larger than the regional average (i.e., the average EP) (Fig. 7). According to the national standard of rainfall grade, it is deemed as rainstorm and heavy rainstorm when the 24-h accumulated precipitation reaches 50–99 mm and 100–200 mm, respectively. Based on the non-stationary GEV model, the EP corresponds to the 59-year time series, and the probability of rainstorms in the EP is the frequency of 50–99 mm in the time series. The calculation of other probabilities is similar. In early summer, the probability of rainstorms in the common EP is zero in Northeast China, which does not suggest that the occurrence of rainstorms is impossible. In mid-summer, rainstorms can occur in most of Northeast China, especially in Liaoning Province, which has a greater than 0.7 possibility. This is mainly influenced by the Bohai Sea and Liaohe River basins. During early summer, the rainstorm probability in the rare EP is above 0.8 in most of Northeast China. In Chifeng City, and the southern part of Northeast China, the probability of heavy rainstorms is above 0.7. The southern and western parts of Northeast China have a high probability of exceeding the average EP. In mid-summer, the probability of the rare EP over rainstorms in the northern and northwestern parts reaches 0.7 and above, and the probability of heavy rainstorms is 0.7 and above in most of Northeast China. In Liaoning Province, Tongliao City, and Chifeng City, the

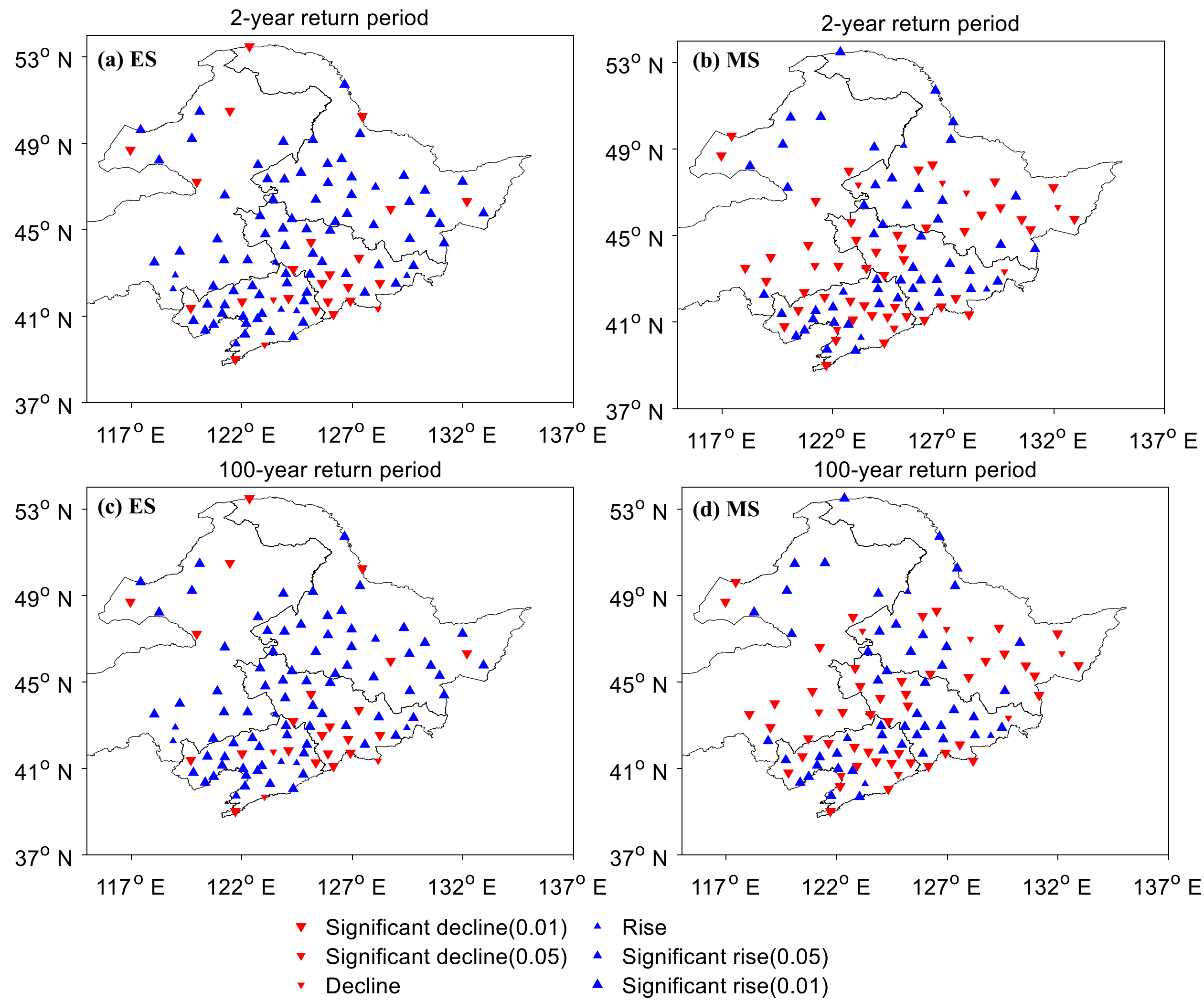

Fig. 6 Spatial distributions of the MK trend analysis method for **a**, **b** the common EP and **c**, **d** the rare EP in **a**, **c** early summer (ES) and **b**, **d** mid-summer (MS). The blue triangle represents an upward trend, while the red triangle represents a downward trend

probability of exceeding the average EP reaches 0.7 and above. In general, the rare EP is dominated by rainstorms in early summer and heavy rainstorms in mid-summer. Note that common EP occurs frequently in Liaoning Province, and the rare EP is more likely to occur in Jilin Province and Heilongjiang Province. The EP values in Liaoning Province, Tongliao City, and Chifeng City are more than those in the whole region. Specifically, in early summer, influenced by the Bohai Sea, there is a higher risk of heavy rainstorm in Chifeng City and southern Liaoning Province. In addition, both the Bohai Sea and Songhua River Basin have a higher probability of exceeding the average EP, indicating that corresponding risk level warnings and flood prevention designs should be higher than those of other areas. In mid-summer, most of Northeast China is a high-risk area for the rare EP and should be a priority region for future prevention measures. To develop policy strategies for disaster prevention and mitigation in Northeast China, it is necessary to focus on the mid-summer season. The results of this study can provide valuable insights towards achieving this goal.

Relationships between the EP and large-scale circulation

Based on the results in "Trends in the EP" section, the variation trend of the EP in early summer and mid-summer in Northeast China has two turning points from 1959 to 2017. Based on the Kriging interpolation method, we analyzed the relationships between the EP and large-scale circulation to explore the impact of large-scale

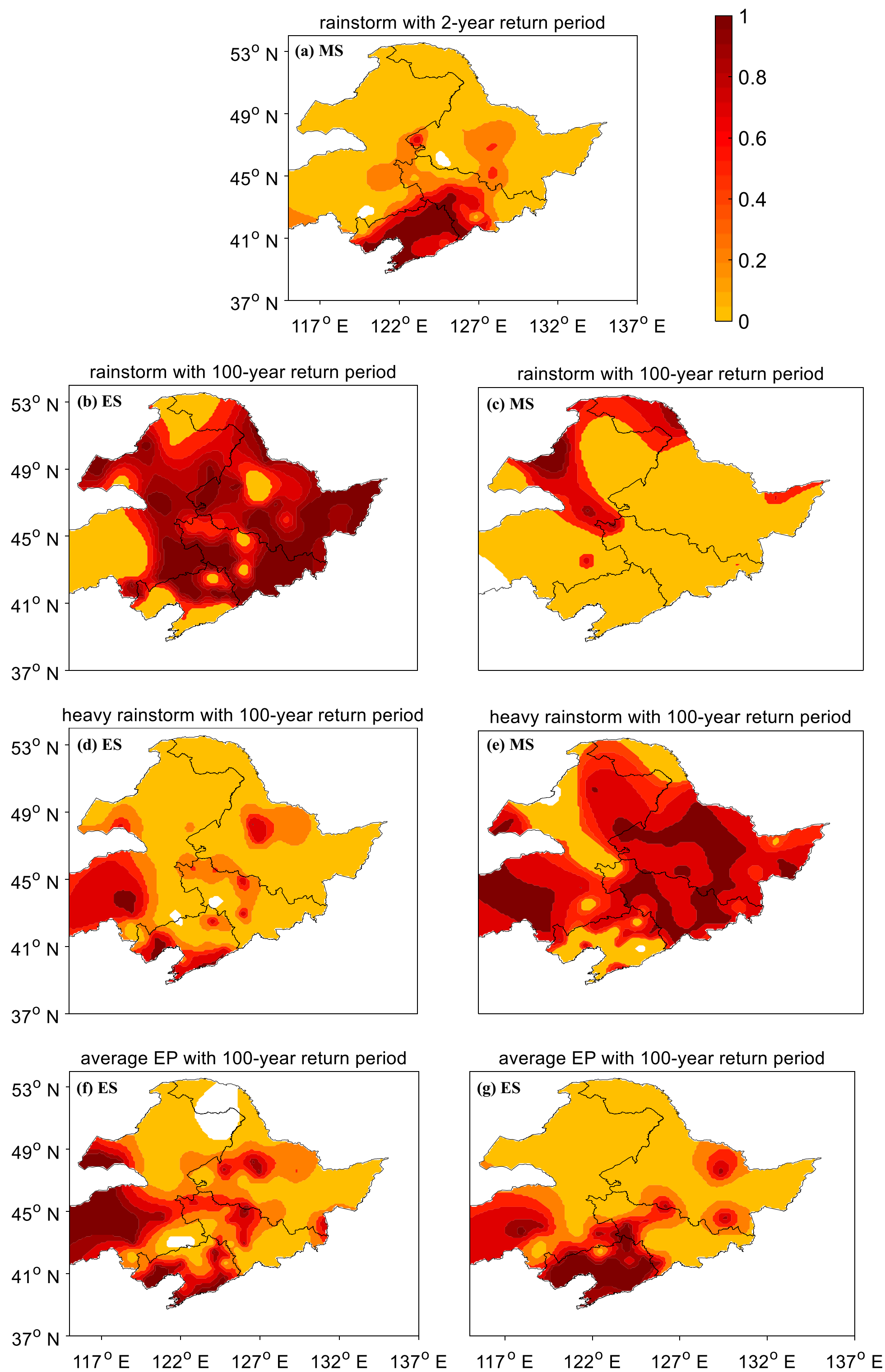

Fig. 7 Probability of **a** the common EP and the rare EP for **b**, **c** rainstorm; **d**, **e** heavy rainstorm; and **f**, **g** the average EP in early summer (ES) and mid-summer (MS)

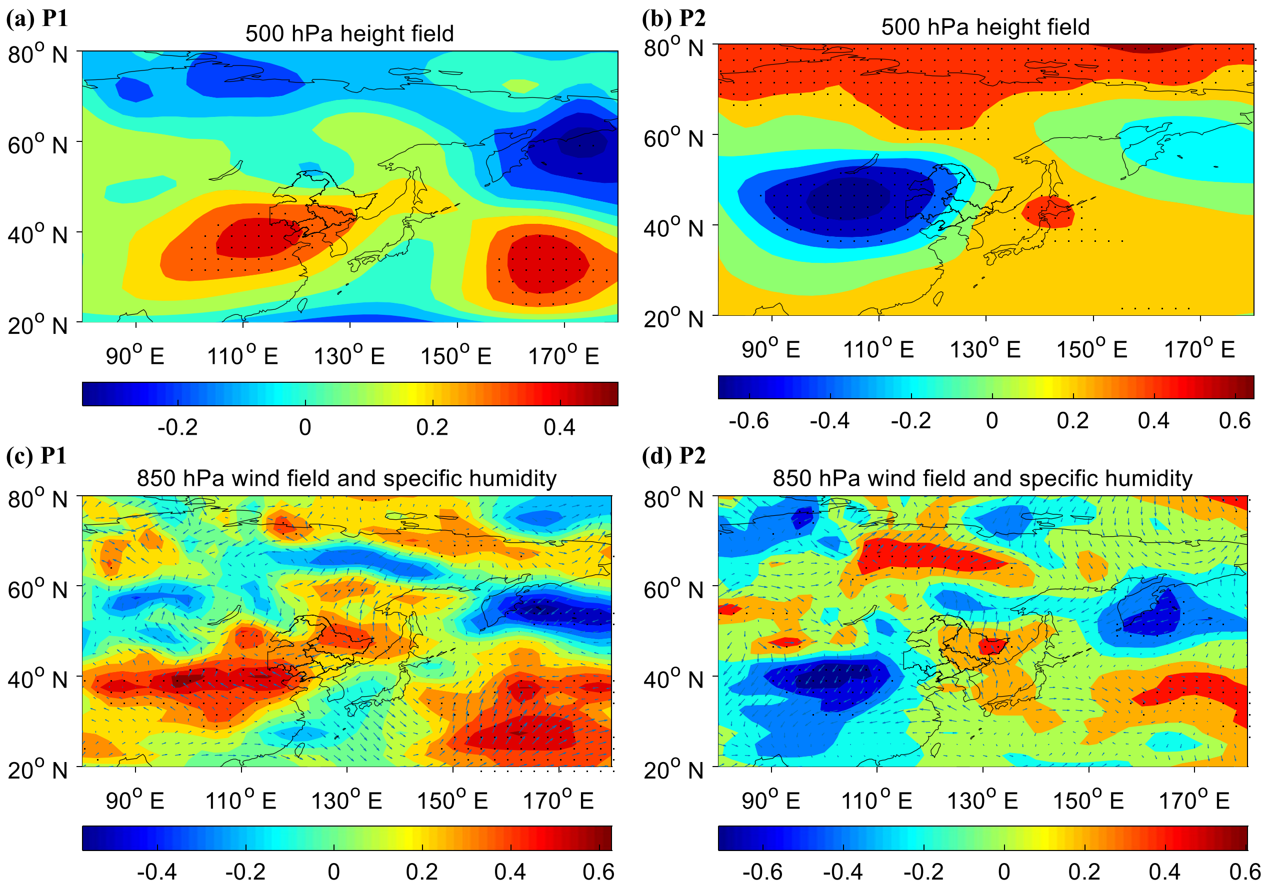

Fig. 8 Correlation coefficients between the EP and **a**, **b** 500 hPa height field; **c**, **d** 850 hPa specific humidity field and wind field in early summer period 1 (P1) and early summer period 2 (P2). The direction of the arrow indicates the wind direction, and the length of the arrow indicates the wind force. Dotting means the correlation coefficients are significant at the 0.05 level

circulation on the EP. According to the mutation years of early and mid-summer (Fig. 2), the early summer is divided into two periods: 1972–1995 (early summer period 1) and 1996–2017 (early summer period 2). Similarly, the mid-summer can also be divided into two periods: 1966–1998 (mid-summer period 1) and 1999–2017 (mid-summer period 2). Figures 8 and 9 show the correlation coefficients between the EP and 500 hPa height field, 850 hPa specific humidity and wind field in early and mid-summer, respectively.

As shown in Figs. 8 and 9, the EP has a significant positive correlation with the height and the specific humidity fields in periods 1 of both early summer and mid-summer, while in periods 2 of both early summer and mid-summer, it is negatively correlated with the height field. In early summer period 1, the EP is mainly affected by the easterly airflow of the anticyclone circulation, which is conducive to the transport of warm-moist air from the sea to Northeast China. In early summer period 2, due to the easterly airflow of the cyclone circulation and the prevailing southerly wind, a large amount of warm-moist air in the Bohai Sea and Yellow Sea are transported northward, leading to the EP events. There is an obvious cyclonic circulation over the northeast, corresponding to the northeast cold vortex on 500 hPa. In mid-summer, the EP is mainly controlled by the temperate anticyclone, and the influence is smaller in mid-summer period 2.

In addition, the MK trend analysis methods of the circulation field are shown in Fig. 10, and significant increasing trends of the height field are detected in both periods. During mid-summer, the range of the height field in the northeast is larger and the cold air and wind in the north are stronger than that in early summer. That means, in mid-summer, cold air is important to the EP in Northeast China, which inhibits the effect of water vapor transportation. Therefore, there is no increasing trend in the EP in mid-summer. On the contrary, in early summer, cold and warm-moist air is active. The warm-moist air moves northward while the cold air moves southward. Thus, the stronger moisture convergence over Northeast China may cause the increase of the EP in early summer.

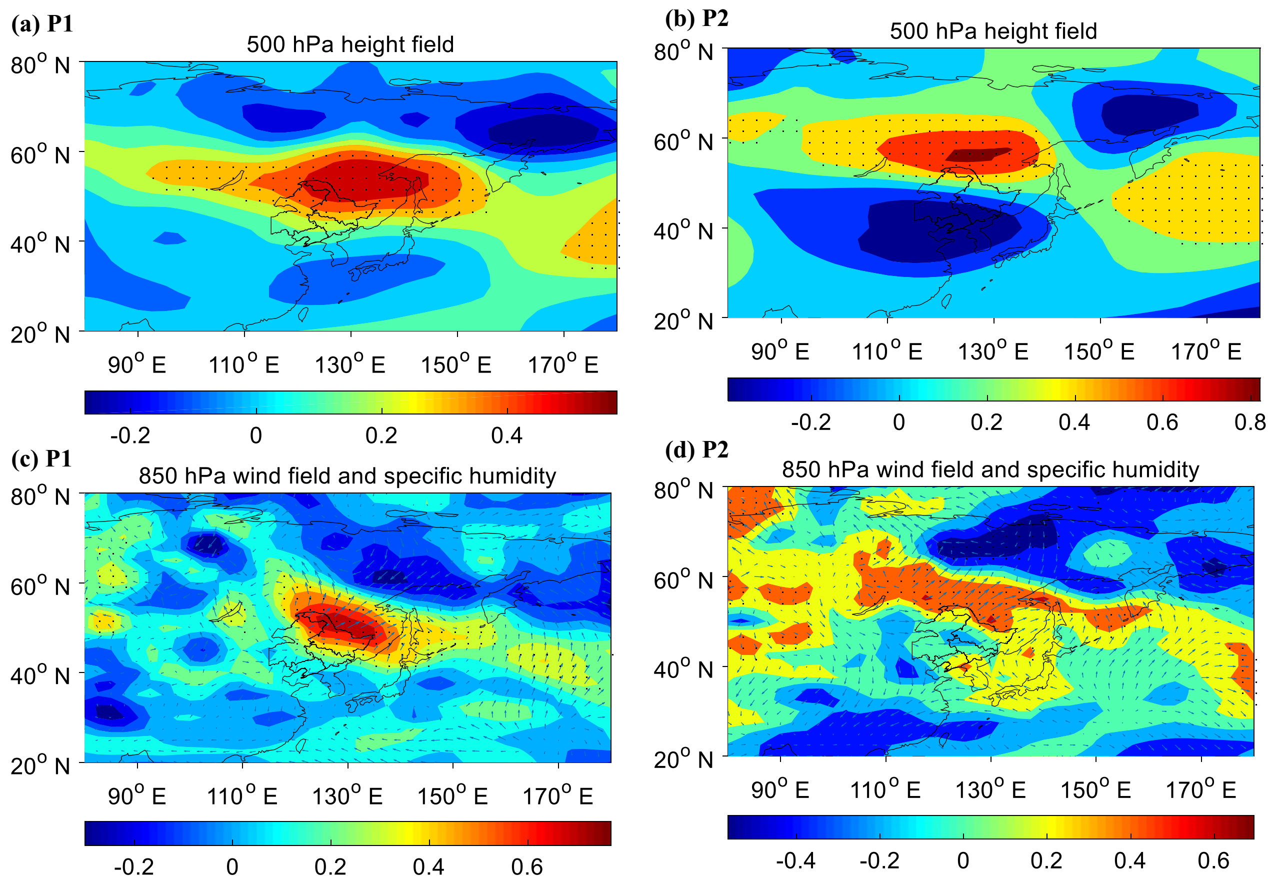

Fig. 9 Correlation coefficients between the EP and **a**, **b** 500 hPa height field; **c**, **d** 850 hPa specific humidity field and wind field in mid-summer period 1 (P1) and mid-summer period 2 (P2). The direction of the arrow indicates the wind direction, and the length of the arrow indicates the wind force. Dotting means the correlation coefficients are significant at the 0.05 level

During the two periods, different characteristics of the circulation field cause the different trends in the EP. The northeast cold vortex is the main influencing system of the EP in early summer (especially in period 2). The stronger moisture convergence over Northeast China is conducive to the increase of the EP in early summer. Nevertheless, the southern part of the temperate anticyclone controls the EP in mid-summer. The cold air is important for the EP in Northeast China, which inhibits the effect of water vapor transport, and thus, the increasing trend of the EP is not obvious in mid-summer. These results are also highly consistent with those in previous studies (Shen et al. 2011; Lin et al. 2021; Wu et al. 2021).

Conclusions

In this study, the MK trend analysis method was applied to detect mutations and the EP trends, and the non-stationary GEV model was used to investigate the trends and potential risks of the EP over Northeast China. Meanwhile, the relationships of non-stationary model parameters to return levels were discussed. Moreover, the impact of large-scale circulation on the EP in Northeast China was investigated. The major findings of this study can be summarized as follows:

1. By using the non-stationary GEV model, all return levels of the EP show increasing trends in early summer, and the growth rate of the EP with 2-year return period is less than that of the EP with 20-, 50-, and 100-year return periods. The results indicate that the EP events are more frequent now. In mid-summer, the EP with 20-, 50-, and 100-year return periods also show slightly increasing trend. Conversely, there is a slightly decreasing trend in the EP with 2-year return period. This phenomenon is caused by the different trends of location parameter u_1 and scale parameter σ_1.
2. In early summer, rainstorm dominates the rare EP in most of Northeast China, especially in Chifeng City, and southeastern Northeast China, which are the key areas for the Northeast cold vortex. Heavy rainstorm prevails in mid-summer, especially in Jilin

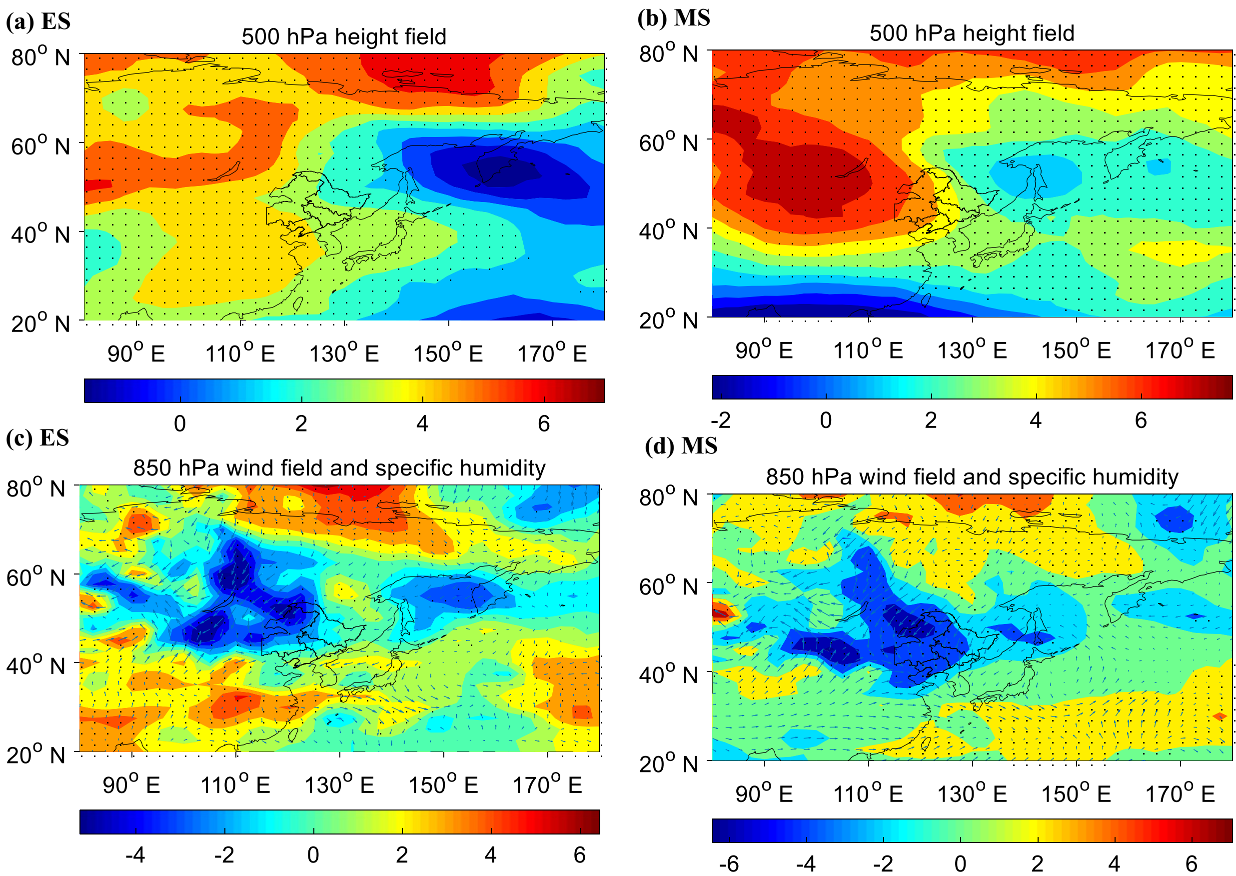

Fig. 10 Spatial distribution of the MK trend analysis method for **a**, **b** 500 hPa height field; **c**, **d** 850 hPa specific humidity field and wind field in early summer (ES) and mid-summer (MS). The direction of the arrow indicates the wind direction, and the length of the arrow indicates the wind force. Dotting means the correlation coefficients at the 0.05 significance level

Province and Heilongjiang Province. The common EP occurs frequently in Liaoning Province, and the rare EP is more likely to occur in Jilin Province and Heilongjiang Province. Besides, both the Bohai Sea and Songhua River Basin have a higher probability of exceeding the average EP, indicating that corresponding risk level warnings and flood prevention designs should be higher than those of other areas. These results may provide a reference for future engineering design.

3. The effect of the Northeast cold vortex on the EP is significant in early summer. The stronger moisture convergence in Northeast China corresponds to the increase of the EP in early summer. However, the southern part of the temperate anticyclone is the main influencing system of the EP in mid-summer. The cold air is important to the EP in Northeast China, inhibiting the effect of water vapor transportation, correspondingly, an increasing trend in the EP is not evident in mid-summer.

Overall, this study comprehensively analyzed the spatiotemporal variability and risk evolution of EP in Northeast China from a new perspective of non-stationary GEV model. The findings in this study can provide references for policy formulation and risk management in this region.

Acknowledgements
We are grateful to the support from the Guangdong Provincial Key Laboratory of Soil and Groundwater Pollution Control and the State Environmental Protection Key Laboratory of Integrated Surface Water-Groundwater Pollution Control.

Author contributions
Conception of the work: Fangxiu Meng, Haiyun Shi. Acquisition of the data: Fangxiu Meng, Kang Xie. Interpretation of the data: Fangxiu Meng, Huazhou Chen, Yao Wang. Supervision: Haiyun Shi. Writing—original draft: Fangxiu Meng. Writing—review and editing: Peng Liu, Haiyun Shi.

Funding
This study was supported by National Natural Science Foundation of China (12161028), Natural Science Foundation of Guangxi Province (2018GXNSFAA050045), and Shenzhen Key Laboratory of Precision Measurement

and Early Warning Technology for Urban Environmental Health Risks (ZDSYS20220606100604008).

Availability of data and materials
The datasets used and/or analyzed in the current study are available from the corresponding author on reasonable request.

Declarations

Competing interests
The authors declare that they have no competing interests.

Received: 7 November 2023 Accepted: 8 March 2024
Published online: 15 March 2024

References
Chen YR, Chu PS (2014) Trends in precipitation extremes and return levels in the Hawaiian Islands under a changing climate. Int J Climatol 34(15):3913–3925
Coles S (2001) An introduction to statistical modeling of extreme values. Springer Verlag, London
Du HB, Wu ZF, Zong SW, Meng XJ, Wang L (2013) Assessing the characteristics of extreme precipitation over NEC using the multifractal detrended fluctuation analysis. J Geophys Res Atmos 118(12):6165–6174
Du M, Zhang J, Yang Q, Wang Z, Bao Z, Liu Y et al (2020) Spatial and temporal variation of rainfall extremes for the North Anhui Province Plain of China over 1976–2018. Nat Hazards 105(3):2777–2797
Fan X, Qin YY, Gao X (2021) Interpretation of the main conclusions and suggestions of IPCC AR6 Working Group I Report. Environ Prot 49(17):1–5
Filliben JJ (1975) The probability plot correlation coefficient test for normality. Technometrics 17(1):111–117
Gao M, Mo DY, Wu XQ (2016) Nonstationary modeling of extreme precipitation in China. Atmos Res 182(15):1–9
García J, Gallego MC, Serrano A, Vaquero J (2007) Trends in block-seasonal extreme rainfall over the Iberian Peninsula in the second half of the twentieth century. J Clim 20(1):113–130
Groisman PY, Knight RW, Karl TR (2001) Heavy precipitation and high streamflow in the contiguous United States: trends in the 20th century. Bull Am Meteor Soc 82(2):1–44
Guan J, Yao J, Li M, Dong L, Zheng JH (2022) Historical changes and projected trends of extreme climate events in Xinjiang. Clim Dyn 59:1753–1774
Guo EL, Zhang JQ, Wang YF, Quan L, Zhang RJ, Zhang F (2019) Spatiotemporal variations of extreme climate events in Northeast China during 1960–2014. Ecol Ind 96:669–683
Han YF, Jiang ZH, Wang J (2005) Temporal and spatial characteristics of summer rainfall in NEC. Meteorol Sci Ogy 33(2):6
Hartmann H, Buchanan H (2014) Trends in extreme precipitation events in the Indus River Basin and flooding in Pakistan. Atmos Ocean 52(1):77–91
IPCC (2021) Climate change 2021: the physical science basis. In: Fox-Kemper B, Hewitt HT, Xiao C et al (eds) Ocean, Cryosphere and sea level change. Cambridge University Press, Cambridge, p 23
Jeon JJ, Sung JH, Chung ES (2016) Abrupt change point detection of annual maximum precipitation using fused lasso. J Hydrol 538:831–841
Jiang ZP, Shi HY, Liu SN, Zhou ZQ, Wang Y, Cai HJ (2021) Evolution characteristics of potential evapotranspiration over the Three-River Headwaters Region. Hydrol Sci J 66(10):1552–1566
Jiang XC, Zhang J, Lei XH (2023) Spatial-temporal variations of extreme precipitation indices in the Xinjiang cold area over the past 60 years. J Hydrol Eng 28(4):04023005
Katz RW (2013) Statistical methods for nonstationary extremes. Springer, London. https://doi.org/10.1007/978-94-007-4479-02
Kendall M (1975) Rank correlation methods, vol 8, 4th edn. Charles Griffin, San Francisco, p 875
Kharin VV, Zwiers FW (2005) Estimating extremes in transient climate change simulations. J Clim 18(8):1156–1173
Li SF, Lian Y, Chen SB, Sun QH, Yao YX (2012) Distribution of extreme cool events over Northeast China in early summer and the related dynamical processes. Scientia Geographica Sinica 32(6):752–758
Lin YT, Zhao CY, Fang YH, Li Q, Fang X et al (2021) Analysis of spatial-temporal variation characteristics and atmosphere circulation factors of precipitation in early and mid-summer in Northeast China. J Meteorol Environ 37(5):63–71
Liu B, Xu M, Henderson M, Qi Y (2005) Observed trends of precipitation amount, frequency, and intensity in China, 1960–2000. J Geophys Res Atmos 110(8):1–10
Mann HB (1945) Nonparametric tests against trend. Econometr J Econometr Soc 3(3):245–259
Ren YY, Ren GY, Sun XB, Shrestha AB, You QL, Zhan YJ et al (2017) Observed changes in surface air temperature and precipitation in the Hindu Kush Himalayan region over the last 100-plus years. Adv Clim Chang Res 8(3):148–156
Roy SS, Balling RC (2004) Trends in extreme daily precipitation indices in India. Int J Climatol 24(4):457–466
Sheikh MM, Manzoor N, Ashraf J, Adnan M, Collins D, Hameed S et al (2015) Trends in extreme daily rainfall and temperature indices over South Asia. Int J Climatol 35(7):1625–1637
Shen BZ, Lin ZD, Lu RY, Lian Y (2011) Circulation anomalies associated with inter-annual variation of early- and late-summer precipitation in NEC. Sci China Earth Sci 54(7):1095–1104
Shi HY, Li TJ, Wei JH (2017) Evaluation of the gridded CRU TS precipitation dataset with the point raingauge records over the Three-River Headwaters region. J Hydrol 548:322–332
Suppiah R, Hennessy KJ (1998) Trends in total rainfall, heavy rain events and number of dry days in Australia, 1910–1990. Int J Climatol 18(10):1141–1164
Tan X, Shao D (2017) Precipitation trends and teleconnections identified using quantile regressions over Xinjiang, China. Int J Climatol 37(3):1510–1525
Wang BL, Zhang MJ, Wei JL, Wang SJ, Li XF, Li SS et al (2013) Changes in extreme precipitation over Northeast China, 1960–2011. Quatern Int 298:177–186
Wang Y, Liu SN, Chen J, Zhou ZQ, Shi HY (2022) Investigating the spatiotemporal variations of extreme rainfall and its potential driving factors with improved partial wavelet coherence. Front Environ Sci 10:951468
Wei FY (2007) Modern climate statistics diagnosis and prediction technology. Weather Press, Beijing
World Meteorological Organization (2009) Manual on estimation of probable maximum precipitation (PMP). World Meteorological Organization
Wu X, Meng F, Liu P, Zhou J, Liu D, Xie K et al (2021) Contribution of the northeast cold vortex index and multiscale synergistic indices to extreme precipitation over Northeast China. Earth Space Sci 8:e2020EA001435
Xavier ACF, Rudke AP, Fujita T et al (2020) Stationary and non-stationary detection of extreme precipitation events and trends of average precipitation from 1980 to 2010 in the Paraná River basin, Brazil. Int J Climatol 40(2):1197–1212
Yu XY, Ma YY (2022) Spatial and temporal analysis of extreme climate events over Northeast China. Atmosphere 13(8):1197
Zhang LL, Chen XH, Lai RY (2020) Urban signatures of sub-daily extreme precipitation events over a metropolitan region. Atmos Res 246(1):105–204
Zhou BT, Qian J (2021) Changes of weather and climate extremes in the IPCC AR6. Adv Clim Chang Res 17(6):713–718
Zhou ZQ, Shi HY, Fu Q et al (2020) Is the cold region in Northeast China still getting warmer under climate change impact? Atmos Res 237:104864
Zilli MT, Carvalho LM, Liebmann B, Silva Dias MA (2017) A comprehensive analysis of trends in extreme precipitation over southeastern coast of Brazil. Int J Climatol 37(5):2269–2279

Publisher's Note